Memoirs of the Faculty of Engineering, Kyushu University, Vol. 68, No.1, March 2008

Transport Model for Sequential Release of Mn, Fe and As under Anaerobic Soil Water Environment

by

Abdur RAZZAK*, Kenji JINNO**, Yoshinari HIROSHIRO***,
Md. Abdul HALIM**** and Keita ODA*****

(Received February 4, 2008)

Abstract

Groundwater contamination has been rising as a critical issue to be solved. Prediction of distribution and fate of different contaminants need to be obtained prior to designing an appropriate monitoring and remediation scheme. To model bacteria mediated redox processes a one-dimensional, multi-component reactive transport model that accounts for the reaction coupling the major redox elements was presented. Mass transport equation was used to simulate transport processes of different pollutants. For the numerical modelling of mass transport in the mobile phase, the method of characteristics was used considering fundamental geochemical processes. Then, solute transport was coupled to microbially mediated organic carbon degradation. To model a complete redox sequence (aerobic or denitrifiers, Mn(IV)-reduction, Fe(III)-reduction, respiration bacteria of iron and arsenic compounds, and As(V) reduction) five functional bacterial groups (X_1, X_2, X_3, X_4 and X_5) were defined. Microbial growth was assumed to follow Monod type kinetics. The exchange between the different phases (mobile, bio, and matrix) was also considered in this approach. Results from a soil column experiment were used to verify the simulation results of the model. It was concluded that the transport model provides a useful framework for predicting the transport of arsenic in the groundwater aquifer.

Keywords: Redox processes, Reducing environment, Microorganism, Simulation model, Reactive transport

1. Introduction

Aquifer contamination by organic compounds is a widespread environmental problem. One of the most reported compounds is arsenic. The quality of groundwater is a great public interest nowadays. Numerical flow and reactive transport models can be helpful tools in the designing, monitoring and of in predicting long-term effects of contaminant transport. In recent years, interest in understanding the mechanisms and prediction of contaminant transport through aquifer has dramatically increased because of growing evidence and public concern that the groundwater is being used as a major source of water supply.

* Graduate Student, Doctoral course, Department of Urban and Environmental Engineering
** Professor, Department of Urban and Environmental Engineering
*** Associate Professor, Department of Urban and Environmental Engineering
***** Post Doctoral Fellow, Department of Urban and Environmental Engineering
***** Graduate Student, Department of Urban and Environmental Engineering

Microbial processes have a major influence on the fate of arsenic in aquifers[1]. It is necessary to develop a comprehensive reactive transport model that can simultaneously describe microbially-mediated bio-chemical reactions as well as other advection–dispersion processes. However, little work has been directed towards simulating the arsenic reactive transport, considering physical, chemical and biochemical processes in porous media. Previous studies on arsenic reactive transport have considered adsorptive transport under abiotic conditions[2]. Lim et al. (2007) considered the effects of the microbial reaction kinetics but they did not show the microbial effect on the relation of manganese and iron release with arsenic[3]. They verified their results by using column experiment but they did not maintain the natural environment of aquifer for the column.

The main objective of this study is the development, validation and application of a coupled transient finite difference model for contaminant transport in soil aquifer that incorporates the effects of microbially mediated reactions on the contaminant transport for the chemical species of arsenic and other background species. In what follows, the main governing phenomena of miscible contaminant transport including advection, dispersion, molecular diffusion and adsorption are considered together with the effect of the microbially mediated chemical reactions. The arsenic transport equation and the balance equations for flow of water are solved numerically using the finite difference method, subject to prescribed initial and boundary conditions. The developed model is validated by comparing the results with a column experiments. It is shown that the developed model is capable of predicting, with a good accuracy, the variations of the contaminant concentration with time considering the effect of chemical reactions.

2. Model Development

2.1 Conceptual model

The model developed in this study is based on the reactive solute transport and bio-geochemical reaction processes under reducing environment. Three different phases are considered in this model.

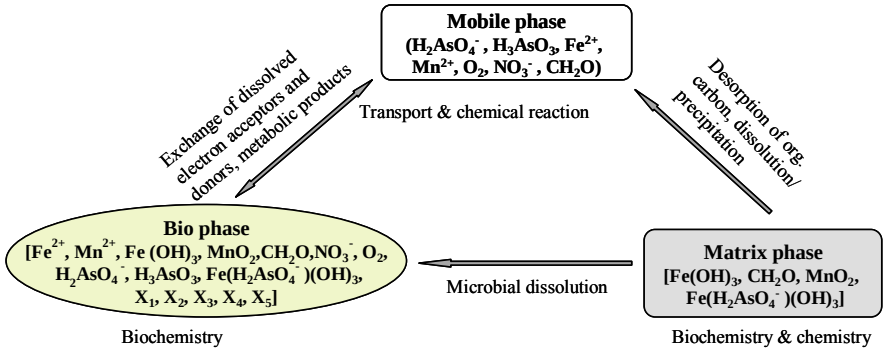

Fig. 1 Conceptual model of the aquifer phases, major processes, exchange relations and species residing in the phases.

The model assumes that the microorganisms reside in an immobile bio phase. The bio phase is commonly called bio-film. All biochemical reactions take place inside the bio phase. The volume of the bio phase is assumed to be constant in time and space and not coupled to microbial growth[4]. Besides the bio phase another two model phases exist; the mobile pore water and the solid matrix phase as shown in **Fig. 1**. The organic compounds can dissolve into the pore water from the aquifer solids. They can also transfer to the bio phase, where they are changed their chemical composition by microbially mediated reactions such as oxidation. Other species involved in the microbial reactions such as electron acceptors reach the bio phase via the pore water (O_2, NO_3^-, $H_2AsO_4^-$) or directly via the aquifer solids (Fe(III), Mn(IV)). The metabolic products (e.g., CO_2, Fe(II)) can further react in the aquifer; however, we do not discuss these processes in the present paper. Five different species of bacteria are assumed to grow in the bio phase. The sequential growth of different species of bacteria is modeled in **Fig. 2**.

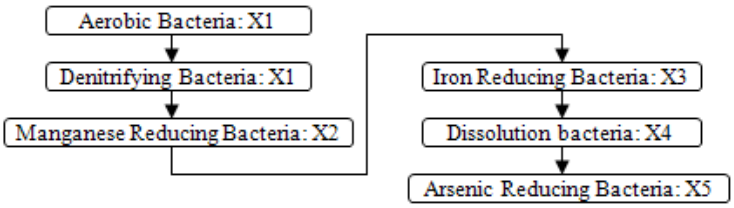

Fig. 2 Sequential growths of different bacteria groups.

2.2 Biochemical reactions and mathematical expression of bacteria growth

The modeling of complex redox sequences requires the consideration of different metabolisms. It also requires the consideration of a variety of substrates, including organic carbons, O_2, NO_3^-, $H_2AsO_4^-$, MnO_2, $Fe(OH)_3$ and $Fe(H_2AsO_4^-)(OH)_3$.

In this model the five functional bacterial groups, bacteria X_1, X_2, X_3, X_4 and X_5 that reside in the immobile bio phase are considered. The bacteria group X_1 uses molecular oxygen under aerobic conditions and NO_3^- under anaerobic conditions as an electron acceptor. Bacteria X_2 uses MnO_2 while bacteria X_3 uses $Fe(OH)_3$ as electron acceptor and bacteria X_4 uses $Fe(H_2AsO_4^-)(OH)_3$ as electron acceptor. Finally bacteria X_5 uses $H_2AsO_4^-$ as electron acceptor for its metabolism reducing it to H_3AsO_3. The bacteria uses dissolved organic carbon chemically defined as CH_2O and the utilizable portion of dead bacteria of 90% as their substrate[5), 6), 7)]. However, bacteria growth is often controlled by availability of substrates.

Microbially mediated redox processes are described by the following reactions[6)]:

***Aerobic respiration* (X_1);**

$$CH_2O + O_2 \rightarrow HCO_3^- + H^+ \quad (1)$$

***Denitrification* (X_1);**

$$5CH_2O + 4NO_3^- \rightarrow 5HCO_3^- + 2N_2 + 2H_2O + H^+ \quad (2)$$

***Manganese dioxide-reduction* (X_2);**

$$CH_2O + 2MnO_2 + 3H^+ \rightarrow HCO_3^- + 2Mn^{2+} + 2H_2O \quad (3)$$

***Iron hydroxide-reduction* (X_3)**;

$$CH_2O + 4Fe(OH)_3 + 7H^+ \rightarrow HCO_3^- + 4Fe^{2+} + 10\,H_2O \quad (4)$$

***Dissolution of co-precipitated Iron-Arsenic* [$Fe(OH)_3(H_2AsO_4^-)$] *reduction* (X_4);**

$$CH_2O + 4Fe(OH)_3(H_2AsO_4^-) + 7H^+ = HCO_3^- + 4Fe^{2+} + 4H_2AsO_4^- + 10H_2O \quad (5)$$

***Arsenic* ($H_2AsO_4^-$)*-reduction* (X_5);**

$$CH_2O + 2H_2AsO_4^- + H^+ = HCO_3^- + 2H_3AsO_3 \quad (6)$$

The growth of bacteria is generally described by the Double Monod kinetic equation[5), 6), 7)] and can be written as follows:

$$\frac{\partial X}{\partial t} = v_{\max} \cdot IT \cdot \frac{C_1}{K_{s1} + C_1} \cdot \frac{C_2}{K_{s2} + C_2} \cdot X \quad (7)$$

where $v_{\max}$ is the maximum growth rate, C_1 is the primary substrate concentration in bio phase, C_2 is the secondary substrate concentration in bio phase, K_{s1} is the primary substrate half-saturation constant, K_{s2} is the secondary substrate half-saturation constant, and X is the bacteria concentration. If the concentrations of all relevant substrates (usually organic carbon and electron acceptors) in the bio phase are high, microorganisms grow exponentially according to the maximum growth rate $v_{\max}$.

Microbial growth can be limited by the inhibition terms. This term was developed by Widdowson et al. (1988)[8)]. This is used to approximate inhibition processes such as the suppression of strictly anaerobic bacteria (X_2, X_3, X_4 and X_5) by the presence of dissolved oxygen. Many aerobic bacteria are facultatively anaerobic (bacteria X_1) and can also grow under denitrifying conditions. The inhibition term can be stated as:

$$IT = \frac{IC}{(IC + C)} \tag{8}$$

IT is the inhibition term for the inhibiting species; *C* is its concentration and *IC* the inhibition constant.

The decay of bacteria equation can be written as:

$$\frac{\partial X}{\partial t} = -v_{dec} \cdot X \tag{9}$$

where v_{dec} is the bacteria decay coefficient.

The model extended to include the switching between aerobic and denitrifying growth conditions is based on the assumption that the same microorganisms are capable of either aerobic or denitrifying growth (bacteria X_1), depending on the oxygen concentration in their nearby environment, and can be written as[6), 9)]:

$$F([O_2]_{bio}) = 0.5 - \frac{1}{\pi}\tan^{-1}\{([O_2]_{bio} - [O_2]_{thres}) \times f_{s1}\} \tag{10}$$

where $F([O_2]_{bio})$ is the switching function, $[O_2]_{bio}$ is the concentration of oxygen O_2 in the bio phase, $[O_2]_{thres}$ is the threshold concentration of oxygen, and f_{s1} is the slope of the switch function.

Microbial growth is accompanied by consumption of substrates. The change of CH_2O concentration in the bio phase is linked to the bacteria growth and the consumption of the organic carbon. For the simplified case of only one bacteria group the total change of organic carbon in the bio phase can be expressed by:

$$\left[\frac{\partial [CH_2O]_{bio}}{\partial t}\right] = -\frac{1}{Y_{OC}}\left[\frac{\partial X}{\partial t}\right]_{growth} - f_{use}\left[\frac{\partial X}{\partial t}\right]_{decay} - \frac{\alpha\theta_w}{\theta_{bio} + \theta_w}([CH_2O]_{bio} - [CH_2]_{mob}) \tag{11}$$

where the yield coefficient Y_{OC} links microbial growth to organic carbon incorporated into cell mass in a given time interval to the total organic carbon consumption[5)]. It is defined as the ratio of organic carbon incorporated into cell mass in a given time interval to the total organic carbon consumption. A part of the organic carbon stored in decaying microbial mass can be reused by the microorganisms. In the model this is simulated by defining an utilizable portion of dead bacteria f_{use}.

The consumption of electron acceptors (e.g. O_2, NO_3^-) is correlated to the organic carbon oxidized for energy gain via stoichiometric relations. The concentration change of a mobile electron acceptor in the bio phase is:

$$\left[\frac{\partial [EA]_{bio}}{\partial t}\right] = -\frac{1}{U_{EA}}\left[\frac{\partial X_1}{\partial t}\right]_{growth} - \frac{\alpha\theta_w}{\theta_{bio} + \theta_w}([EA]_{bio} - [EA]_{mob}) \tag{12}$$

$$U_{EA} = ST.\frac{Y_{OC}}{(1 - Y_{OC})} \tag{13}$$

where *ST* is the stoichiometric coefficient between organic carbon and electron accepter (OC/EA) of the reaction and α is the exchange coefficient to represent the mass transfer between bio and mobile phases through their boundary film. U_{EA} is the utilization factor, θ_w and θ_{bio} are the volumetric fraction of water content for the mobile phase and volumetric fraction of bio phase of soil respectively.

Microbial growth does not only cause the consumption of substrates, but also release its metabolic products. The release of metabolic product is related to microbial growth via a production factor P. The production factor for a given metabolic product is stoichiometrically related to the consumption of an electron acceptor. Thus, the release of the Mn- or the Fe- hydroxides is related to bacteria growth, e.g., Mn-hydroxides:

$$\left[\frac{\partial [Mn^{2+}]_{bio}}{\partial t}\right] = \frac{1}{P_{Mn^{2+}}}\left[\frac{\partial X_2}{\partial t}\right]_{growth} - \frac{\alpha\theta_w}{\theta_{bio}+\theta_w}\left([Mn^{2+}]_{bio} - [Mn^{2+}]_{mob}\right) \quad (14)$$

$$P_{Mn^{2+}} = \frac{1}{2}\cdot\frac{Y_{OC}^{MnO_2}}{(1-Y_{OC}^{MnO_2})} \quad (15)$$

where $P_{Mn^{2+}}$ is the production factor for Mn^{2+} and $Y_{OC}^{MnO_2}$ is the yielding coefficient of MnO_2.

Based on Monod kinetics, the following mathematical equations are formulated for the growth of different groups of bacteria.

Bacteria X_1:

$$\left[\frac{\partial X_1}{\partial t}\right]_{Total\_growth} = \left[\frac{\partial X_1}{\partial t}\right]_{aerobic\_growth} + \left[\frac{\partial X_1}{\partial t}\right]_{denitrifying\_growth} + \left[\frac{\partial X_1}{\partial t}\right]_{decay} \quad (16)$$

where the each term in the right side is expressed as follows;

$$\left[\frac{\partial X_1}{\partial t}\right]_{aerobic\_growth} = \nu_{\max}^{O_2}\cdot\{1-F(O_{2bio})\}\cdot\frac{[CH_2O]_{bio}}{K_{CH_2O}+[CH_2O]_{bio}}\cdot\frac{[O_2]_{bio}}{K_{O_2}+[O_2]_{bio}}\cdot X_1 \quad (17)$$

$$\left[\frac{\partial X_1}{\partial t}\right]_{denitrifying\_growth} = \nu_{\max}^{NO_3^-}\cdot\{F(O_{2bio})\}\cdot\frac{[CH_2O]_{bio}}{K_{CH_2O}+[CH_2O]_{bio}}\cdot\frac{[NO_3^-]_{bio}}{K_{NO_3^-}+[NO_3^-]_{bio}}\cdot X_1 \quad (18)$$

$$\left[\frac{\partial X_1}{\partial t}\right]_{decay} = -\nu_{X_1 dec}\cdot X_1 \quad (19)$$

Bacteria X_2:

Similarly, same expressions are used to model the manganese dioxide-reducing bacteria as follows;

$$\left[\frac{\partial X_2}{\partial t}\right]_{Total\_growth} = \left[\frac{\partial X_2}{\partial t}\right]_{growth} + \left[\frac{\partial X_2}{\partial t}\right]_{decay} \quad (20)$$

$$\left[\frac{\partial X_2}{\partial t}\right]_{growth} = \nu_{\max}^{MnO_2}\cdot\frac{[CH_2O]_{bio}}{K_{CH_2O}+[CH_2O]_{bio}}\cdot\frac{[MnO_2]_{bio}}{K_{MnO_2}+[MnO_2]_{bio}}\cdot X_2 \quad (21)$$

$$\left[\frac{\partial X_2}{\partial t}\right]_{decay} = -\nu_{X_2 dec}\cdot X_2 \quad (22)$$

Bacteria X_3:

$$\left[\frac{\partial X_3}{\partial t}\right]_{Total\_growth} = \left[\frac{\partial X_3}{\partial t}\right]_{growth} + \left[\frac{\partial X_3}{\partial t}\right]_{decay} \quad (23)$$

$$\left[\frac{\partial X_3}{\partial t}\right]_{growth} = \nu_{\max}^{Fe(OH)_3}\cdot\frac{[CH_2O]_{bio}}{K_{CH_2O}+[CH_2O]_{bio}}\cdot\frac{[Fe(OH)_3]_{bio}}{K_{Fe(OH)_3}+[Fe(OH)_3]_{bio}}\cdot X_3 \quad (24)$$

$$\left[\frac{\partial X_3}{\partial t}\right]_{decay} = -\nu_{X_3 dec}\cdot X_3 \quad (25)$$

Bacteria X_4:

$$\left[\frac{\partial X_4}{\partial t}\right]_{Total\_growth} = \left[\frac{\partial X_4}{\partial t}\right]_{growth} + \left[\frac{\partial X_4}{\partial t}\right]_{decay} \quad (26)$$

$$\left[\frac{\partial X_4}{\partial t}\right]_{growth} = \nu_{\max}^{Fe(H_2AsO_4^-)(OH)_3} \cdot \frac{IC_{Fe(OH)_3}}{IC_{Fe(OH)_3} + [Fe(OH)_3]_{bio}} \cdot \frac{[CH_2O]_{bio}}{K_{CH_2O} + [CH_2O]_{bio}} \cdot \frac{[Fe(H_2AsO_4^-)(OH)_3]_{bio}}{K_{Fe(H_2AsO_4^-)(OH)_3} + [Fe(H_2AsO_4^-)(OH)_3]_{bio}} \cdot X_4 \quad (27)$$

$$\left[\frac{\partial X_4}{\partial t}\right]_{decay} = -\nu_{X_4 dec} \cdot X_4 \quad (28)$$

Bacteria X_5:

$$\left[\frac{\partial X_5}{\partial t}\right]_{Total\_growth} = \left[\frac{\partial X_5}{\partial t}\right]_{growth} + \left[\frac{\partial X_5}{\partial t}\right]_{decay} \quad (29)$$

$$\left[\frac{\partial X_5}{\partial t}\right]_{growth} = \nu_{\max}^{H_2AsO_4^-} \cdot \frac{[CH_2O]_{bio}}{K_{CH_2O} + [CH_2O]_{bio}} \cdot \frac{[H_2AsO_4^-]_{bio}}{K_{H_2AsO_4^-} + [H_2AsO_4^-]_{bio}} \cdot X_5 \quad (30)$$

$$\left[\frac{\partial X_5}{\partial t}\right]_{decay} = -\nu_{X_5 dec} \cdot X_5 \quad (31)$$

2.3 Model equations in mobile, bio and matrix phases

The chemical part of the model incorporates all reactions for the chemical species that are considered as shown in **Table 1**. The equations are constructed by mass balances in each phase. In principle all chemical process are time dependent.

Table 1 Chemical species considered in the model.

Mobile phase	$H_2AsO_4^-$, H_3AsO_3, Fe^{2+}, Mn^{2+}, O_2, NO_3^-, CH_2O
Bio Phase	Fe^{2+}, Mn^{2+}, NO_3^-, $Fe(OH)_3$, MnO_2, O_2, CH_2O, $H_2AsO_4^-$, H_3AsO_3, $Fe(H_2AsO_4^-)(OH)_3$
Bacteria	X_1, X_2, X_3, X_4, X_5
Soil matrix phase	$Fe(OH)_3$, MnO_2, CH_2O, $Fe(H_2AsO_4^-)(OH)_3$

The model considered the concentration changes of the species in three different phases. The concentration change in mobile phase includes advection, dispersion, mass transfer between mobile and bio phases, and mass transfer between the mobile and matrix phases. The concentration change in bio phase is result of reduction reaction by the bacteria growth which is mentioned previously, mass transfer between mobile and bio phases, and mass transfer between bio and matrix phases. The concentration change in matrix phase is result of mass transfer between the bio and matrix phases, and mass transfer between the mobile and matrix phases.

As described in the conceptual model, dissolved Fe(II) concentration is simultaneously affected by abiotic microbial reduction of Fe (III) from iron oxy-hydroxide and dissolution of Fe-As compound. Cummings et al. (1999)[10] showed that the dissimilatory iron-reducer promotes arsenate (As(V)) mobilization from As-contaminated sediments. Respiratory reduction of Fe(III) to Fe(II) accounted for arsenic mobilization, as no reduction of As(V) to As(III) occurred. Fe(II) concentration changes depend on the activity of bacteria X_3 and X_4. It is the summation of Fe(II) release by the iron reducing bacteria X_3 as well as by the respiration bacteria X_4 when they use $Fe(OH)_3$ and $Fe(OH)_3(H_2AsO_4^-)$ as their substrate, respectively. This process is modeled by the two terms on the right side of eq. (45) as shown below. Bacteria X_4 also releases As(V) to the bio phase. Under reducing condition, As(V)-reducing bacteria would respire dissolved As(V), with its conversion to As(III)[11]. As(V) concentration change depends on the activity of bacteria X_4 and X_5. Bacteria X_4 releases As(V) as their metabolic product and bacteria X_5 utilize As(V) for their

metabolism to release As(III). In eq. (46), first term indicates that the As(V) release by bacteria X_4 by using Fe-As compound as their substrate and second term indicates that the arsenic reducing bacteria X_5 utilizes As(V) to reduce it to As(III).

Based on the model processes, transport of species in mobile phase can be written as:

Mobile phase; Equation of advection, dispersion with chemical reaction term;

O_2:

$$\frac{\partial [O_2]_{mob}}{\partial t} + \bar{v}\frac{\partial [O_2]_{mob}}{\partial x} = D_L \frac{\partial^2 [O_2]_{mob}}{\partial x^2} + \frac{\alpha\theta_{bio}}{\theta_{bio}+\theta_w}\left([O_2]_{bio} - [O_2]_{mob}\right) \tag{32}$$

NO_3^-:

$$\frac{\partial [NO_3^-]_{mob}}{\partial t} + \bar{v}\frac{\partial [NO_3^-]_{mob}}{\partial x} = D_L \frac{\partial^2 [NO_3^-]_{mob}}{\partial x^2} + \frac{\alpha\theta_{bio}}{\theta_{bio}+\theta_w}\left([NO_3^-]_{bio} - [NO_3^-]_{mob}\right) \tag{33}$$

Mn^{2+}:

$$\frac{\partial [Mn^{2+}]_{mob}}{\partial t} + \bar{v}\frac{\partial [Mn^{2+}]_{mob}}{\partial x} = D_L \frac{\partial^2 [Mn^{2+}]_{mob}}{\partial x^2} + \frac{\alpha\theta_{bio}}{\theta_{bio}+\theta_w}\left([Mn^{2+}]_{bio} - [Mn^{2+}]_{mob}\right) \tag{34}$$

Fe^{2+}:

$$\frac{\partial [Fe^{2+}]_{mob}}{\partial t} + \bar{v}\frac{\partial [Fe^{2+}]_{mob}}{\partial x} = D_L \frac{\partial^2 [Fe^{2+}]_{mob}}{\partial x^2} + \frac{\alpha\theta_{bio}}{\theta_{bio}+\theta_w}\left([Fe^{2+}]_{bio} - [Fe^{2+}]_{mob}\right) \tag{35}$$

CH_2O:

$$\begin{aligned}\frac{\partial [CH_2O]_{mob}}{\partial t} + \bar{v}\frac{\partial [CH_2O]_{mob}}{\partial x} = {} & D_L \frac{\partial^2 [CH_2O]_{mob}}{\partial x^2} \\ & + \frac{\alpha\theta_{bio}}{\theta_{bio}+\theta_w}\left([CH_2O]_{bio} - [CH_2O]_{mob}\right) \\ & + \frac{\beta\theta_{mat}}{\theta_{mat}+\theta_w}\left([CH_2O]_{mat} - [CH_2O]_{mob}\right)\end{aligned} \tag{36}$$

$H_2AsO_4^-$:

$$\begin{aligned}\frac{\partial [H_2AsO_4^-]_{mob}}{\partial t} + \bar{v}\frac{\partial [H_2AsO_4^-]_{mob}}{\partial x} = {} & D_L \frac{\partial^2 [H_2AsO_4^-]_{mob}}{\partial x^2} \\ & + \frac{\alpha\theta_{bio}}{\theta_{bio}+\theta_w}\left([H_2AsO_4^-]_{bio} - [H_2AsO_4^-]_{mob}\right)\end{aligned} \tag{37}$$

H_3AsO_3:

$$\begin{aligned}\frac{\partial [H_3AsO_3]_{mob}}{\partial t} + \bar{v}\frac{\partial [H_3AsO_3]_{mob}}{\partial x} = {} & D_L \frac{\partial^2 [H_3AsO_3]_{mob}}{\partial x^2} \\ & + \frac{\alpha\theta_{bio}}{\theta_{bio}+\theta_w}\left([H_3AsO_3]_{bio} - [H_3AsO_3]_{mob}\right)\end{aligned} \tag{38}$$

where β is the exchange coefficient to represent the mass transfer between matrix and mobile phases through their boundary film.

Bio phase;

(1) Equation of electron accepter:

O_2:

$$\frac{\partial [O_2]_{bio}}{\partial t} = -\frac{1}{U_{O_2}}\left[\frac{\partial X_1}{\partial t}\right]_{aerobic\_growth} - \frac{\alpha\theta_w}{\theta_{bio}+\theta_w}\left([O_2]_{bio} - [O_2]_{mob}\right) \tag{39}$$

NO_3^-:

$$\frac{\partial [NO_3^-]_{bio}}{\partial t} = -\frac{1}{U_{NO_3^-}}\left[\frac{\partial X_1}{\partial t}\right]_{denitrifying\_growth} - \frac{\alpha\theta_w}{\theta_{bio}+\theta_w}\left([NO_3^-]_{bio} - [NO_3^-]_{mob}\right) \tag{40}$$

MnO_2:

$$\frac{\partial [MnO_2]_{bio}}{\partial t} = -\frac{1}{U_{MnO_2}}\left[\frac{\partial X_2}{\partial t}\right]_{growth} - \frac{\gamma\theta_{mat}}{\theta_{bio}+\theta_{mat}}\left([MnO_2]_{bio} - [MnO_2]_{mat}\right) \tag{41}$$

$Fe(OH)_3$:

$$\frac{\partial [Fe(OH)_3]_{bio}}{\partial t} = -\frac{1}{U_{Fe(OH)_3}}\left[\frac{\partial X_3}{\partial t}\right]_{growth} - \frac{\gamma\theta_{mat}}{\theta_{bio}+\theta_{mat}}\left([Fe(OH)_3]_{bio} - [Fe(OH)_3]_{mat}\right) \tag{42}$$

$Fe(H_2AsO_4^-)(OH)_3$:

$$\frac{\partial [Fe(H_2AsO_4^-)(OH)_3]_{bio}}{\partial t} = -\frac{1}{U_{Fe(H_2AsO_4^-)(OH)_3}}\left[\frac{\partial X_5}{\partial t}\right]_{growth} - \frac{\gamma\theta_{mat}}{\theta_{bio}+\theta_{mat}}\left([Fe(H_2AsO_4^-)(OH)_3]_{bio} - [Fe(H_2AsO_4^-)(OH)_3]_{mat}\right) \tag{43}$$

where γ is the exchange coefficient to represent the mass transfer between bio and matrix phases through their boundary film.

(2) Reduced ions in bio phase as a result of bacteria mediated reaction and transfer from mobile phase:

Mn^{2+}:

$$\frac{\partial [Mn^{2+}]_{bio}}{\partial t} = \frac{1}{P_{Mn^{2+}}}\left[\frac{\partial X_2}{\partial t}\right]_{growth} - \frac{\alpha\theta_w}{\theta_{bio}+\theta_w}\left([Mn^{2+}]_{bio} - [Mn^{2+}]_{mob}\right) \tag{44}$$

Fe^{2+}:

$$\frac{\partial [Fe^{2+}]_{bio}}{\partial t} = \frac{1}{P_{Fe^{2+}}}\left[\frac{\partial X_3}{\partial t}\right]_{growth} + \frac{1}{P_{Fe^{2+}}}\left[\frac{\partial X_4}{\partial t}\right]_{growth} - \frac{\alpha\theta_w}{\theta_{bio}+\theta_w}\left([Fe^{2+}]_{bio} - [Fe^{2+}]_{mob}\right) \tag{45}$$

$H_2AsO_4^-$:

$$\frac{\partial [H_2AsO_4^-]_{bio}}{\partial t} = \frac{1}{P_{H_2AsO_4^-}}\left[\frac{\partial X_4}{\partial t}\right]_{growth} - \frac{1}{U_{H_2AsO_4^-}}\left[\frac{\partial X_5}{\partial t}\right]_{growth} - \frac{\alpha\theta_w}{\theta_{bio}+\theta_w}\left([H_2AsO_4^-]_{bio} - [H_2AsO_4^-]_{mob}\right) \tag{46}$$

H_3AsO_3:

$$\frac{\partial [H_3AsO_3]_{bio}}{\partial t} = \frac{1}{P_{H_3AsO_3}}\left[\frac{\partial X_5}{\partial t}\right]_{growth} - \frac{\alpha\theta_w}{\theta_{bio}+\theta_w}\left([H_3AsO_3]_{bio} - [H_3AsO_3]_{mob}\right) \tag{47}$$

(3) Change of organic carbon in bio phase corresponding bacteria growth including reuse of dead body, and transfer from mobile and matrix phases:

CH_2O:

$$\begin{aligned}\frac{\partial [CH_2O]_{bio}}{\partial t} = & -\frac{1}{Y_{CH_2O}^{O_2}}\left[\frac{\partial X_1}{\partial t}\right]_{aerobic\ condition} - \frac{1}{Y_{CH_2O}^{NO_3^-}}\left[\frac{\partial X_1}{\partial t}\right]_{denitrifyi\ ng\ condition} \\ & - \frac{1}{Y_{CH_2O}^{MnO_2}}\left[\frac{\partial X_2}{\partial t}\right]_{growth} - \frac{1}{Y_{CH_2O}^{Fe(OH)_3}}\left[\frac{\partial X_3}{\partial t}\right]_{growth} \\ & - \frac{1}{Y_{CH_2O}^{Fe(H_2AsO_4^-)(OH)_3}}\left[\frac{\partial X_4}{\partial t}\right]_{growth} - \frac{1}{Y_{CH_2O}^{H_3AsO_3}}\left[\frac{\partial X_5}{\partial t}\right]_{growth} \\ & + \sum_{i-1}^{5} f_{use}\cdot v_{decay}\cdot X_1 - \frac{\gamma\theta_{mat}}{\theta_{bio}+\theta_{mat}}\left([CH_2O]_{bio} - [CH_2O]_{mat}\right) \\ & - \frac{\alpha\theta_w}{\theta_{bio}+\theta_w}\left([CH_2O]_{bio} - [CH_2O]_{mob.}\right)\end{aligned} \tag{48}$$

Matrix phase;

MnO_2:

$$\frac{\partial [MnO_2]_{mat}}{\partial t} = \frac{\gamma\theta_{bio}}{\theta_{bio}+\theta_{mat}}\left([MnO_2]_{bio} - [MnO_2]_{mat}\right) \tag{49}$$

$Fe(OH)_3$:

$$\frac{\partial [Fe(OH)_3]_{mat}}{\partial t} = \frac{\gamma\theta_{bio}}{\theta_{bio}+\theta_{mat}}\left([Fe(OH)_3]_{bio} - [Fe(OH)]_{mat}\right) \tag{50}$$

CH_2O:

$$\begin{aligned}\frac{\partial [CH_2O]_{mat}}{\partial t} = & \frac{\gamma\theta_{bio}}{\theta_{bio}+\theta_{mat}}\left([CH_2O]_{bio} - [CH_2O]_{mat}\right) \\ & + \frac{\beta\theta_w}{\theta_{mat}+\theta_w}\left([CH_2O]_{mob} - [CH_2O]_{mat}\right)\end{aligned} \tag{51}$$

$Fe(H_2AsO_4^-)(OH)_3$:

$$\frac{\partial [Fe(H_2AsO_4^-)(OH)_3]_{mat}}{\partial t} = \frac{\gamma\theta_{bio}}{\theta_{bio}+\theta_{mat}}\left([Fe(H_2AsO_4^-)(OH)_3]_{bio} - [Fe(H_2AsO_4^-)(OH)_3]_{mat}\right) \tag{52}$$

3. Verification of the Developed Model; Algorithm of Numerical Simulation and Column Experiment

3.1 Algorithm of numerical simulation and calculation condition

In this model, the whole equation system describing transport, biochemical reactions, chemical equilibrium and chemical kinetics reactions are solved simultaneously. The method of characteristics and the finite difference schemes have been used as numerical solution techniques to solve the model equations. A sequential procedure is used where first the advection and dispersion transport equations are solved explicitly for each chemical species. The source /sink terms accounting for reactions are taken from the preceding time step. Then the chemical and biochemical reaction equations are solved with the concentration changes from the transport step as explicit source/sink terms. The exchange processes between the different model phases are also calculated in the biochemical reaction step. The general procedures performed in model for a typical simulation is shown in **Fig. 3**.

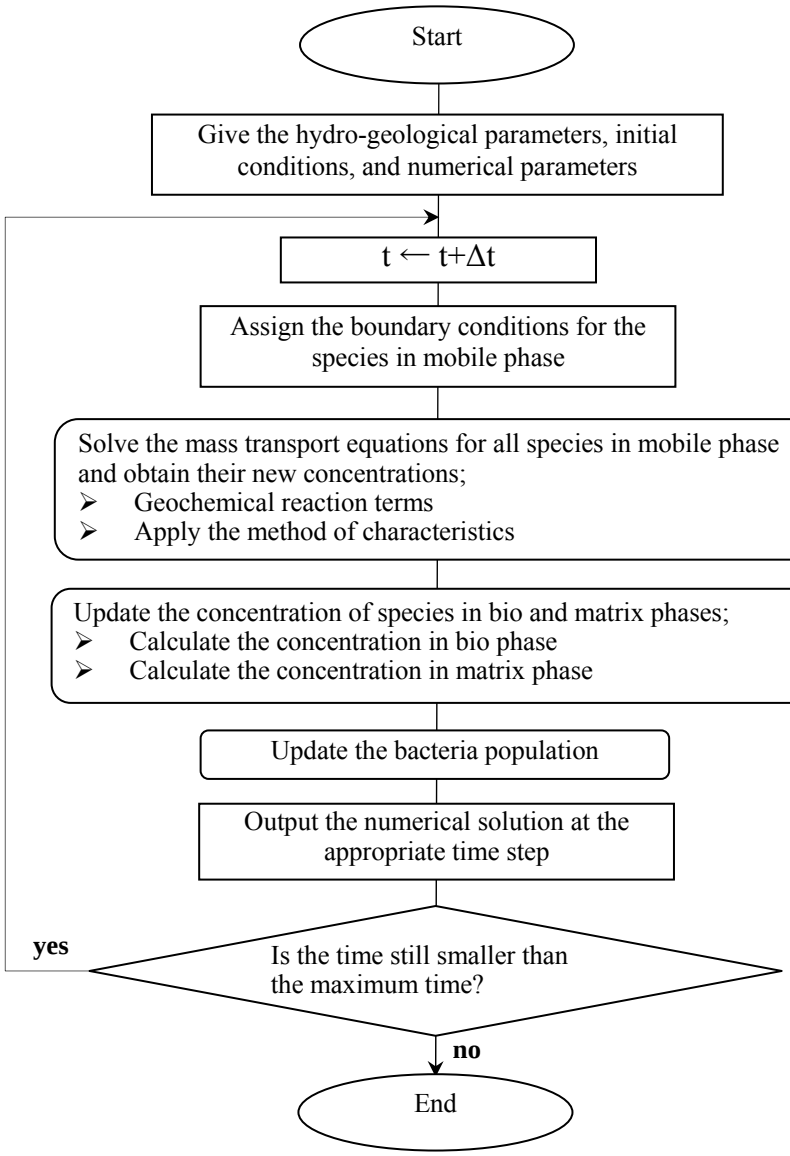

Fig. 3 Illustration of the flow chart for simulating the arsenic transport in groundwater.

The biochemical parameters, and exchange parameters used in this model are displayed in **Table 2**. Monod kinetic, stoichiometric and switching function parameters were taken from several studies related to biochemical simulation[5), 7)]. Some parameters (e.g. maximum growth rate of bacteria) were adjusted by trial and error to obtain the best fit of the model to the experimental data. The initial and boundary conditions were selected depending on the experimental set-up, injection water analysis and chemical components of soils. The initial and boundary conditions are given in **Table 3**. **Table 4** shows the calculation condition.

Table 2 Parameters used for the simulation.

Biochemical parameter		Parameter values
Exchange coefficient	Bio-Mobile: α[12)]	10.00000 day^{-1}
	Bio-Matrix: β[12),13)]	0.00500day^{-1}
	Matrix-Mobile: γ[12),13)]	0.00005day^{-1}
Monod half velocity	K_{CH_2O}[7)], K_{O_2}[7)], $K_{NO_3^-}$,[7)] $K_{H_2AsO_4^-}$[7)], K_{MnO_2}[7)], $K_{Fe(OH)_3}$[7)]	0. 10000 mmol L^{-1}
		0.00100 mmol L^{-1}
	$K_{Fe(H_2AsO_4^-)(OH)_3}$[Δ]	0.010 mmol L^{-1}
Aerobic bacteria X_1	Yield Coefficient $Y_{CH_2O}^{O_2}$[7)]	0.10000 mol cell-C/mol OC
	Maximum growth rate $\nu_{\max}^{O_2}$[7)]	3.00000 day^{-1}
	Constant decay rate $\nu_{X_1 dec}$[7)]	0.30000 day^{-1}
Anaerobic bacteria X_1	Yield Coefficient $Y_{CH_2O}^{NO_3^-}$[*]	0.09800 mol cell-C/mol OC
	Maximum growth rate $\nu_{\max}^{NO_3^-}$[*]	1.12500 day^{-1}
	Constant decay rate $\nu_{X_1 dec}$	0.11250 day^{-1}
Mn reducing bacteria X_2	Yield Coefficient $Y_{CH_2O}^{MnO_2}$[*]	0.23000 mol cell-C/mol OC
	Maximum growth rate $\nu_{\max}^{MnO_2}$[*]	0.36000 day^{-1}
	Constant decay rate $\nu_{X_2 dec}$	0.03600 day^{-1}
Fe reducing bacteria X_3	Yield Coefficient $Y_{CH_2O}^{Fe(OH)_3}$[*]	0.21000 mol cell-C/mol OC
	Maximum growth rate $\nu_{\max}^{Fe(OH)_3}$[*]	0.75000day^{-1}
	Constant decay rate $\nu_{X_3 dec}$	0.02500 day^{-1}
Dissolution bacteria X_4	Yield Coefficient $Y_{CH_2O}^{Fe(H_2AsO_4^-)(OH)_3}$[Δ]	0.01000 mol cell-C/mol OC
	Maximum growth rate $\nu_{\max}^{Fe(H_2AsO_4^-)(OH)_3}$[Δ]	0.89000 day^{-1}
	Constant decay rate $\nu_{X_4 dec}$[Δ]	0.08900 day^{-1}
As reducing bacteria X_5	Yield Coefficient $Y_{CH_2O}^{H_2AsO_4^-}$[Δ]	0.01000 mol cell-C/mol OC
	Maximum growth rate $\nu_{\max}^{H_2AsO_4^-}$[Δ]	0.10000 day^{-1}
	Constant decay rate $\nu_{X_5 dec}$[Δ]	0.01000 day^{-1}
Switching function	Threshold concentration of O_2: $[O_2]_{thres}$[13)]	0.01500 mmol L^{-1}
	Slope of switch function f_{s1}[13)]	40.00000
Specific volume	Mobile phase: θ_w	0.30000
	Bio phase: θ_w[7)]	0.02000
	Matrix phase: θ_w	0.68000

[Δ] By the authors
[*] Tuned by the authors

Table 3 Initial and boundary conditions.

Chemical species	Boundary condition (injection water) (mmol L^{-1})	Initial concentration		
		Mobile phase (mmol L^{-1})	Bio phase (mmol L^{-1})	Matrix phase (mg kg^{-1})
DO	0.44	0.0938	0.0938	0.0
NO_3^-	0.00065	0.0	0.0	0.0
CH_2O	0.0	0.526	0.526	0.0
H_3AsO_3	0.0	0.0	0.0	4.972
$H_2AsO_4^-$	0.0000231	0.0000085	0.0000085	0.0
Fe^{2+}	0.0000286	0.0013	0.0013	0.0
Mn^{2+}	0.0000419	0.00699	0.00699	0.0
$Fe(OH)_3$		0.0	0.0	79334.32
MnO_2		0.0	0.0	1707.90
$Fe(H_2AsO_4)(OH)_3$		0.0	0.0	32.48

Table 4 Calculation conditions.

Calculation depth	30 cm
Calculation period	23 days
Grid mesh size	0.60000 cm
Time increment	10 sec
Pore water velocity	0.00001 cms^{-1}
Porosity	0.30000
Longitudinal dispersion length	0.02000 cm

3.2 Column experiment

A one-dimensional column experiment was carried out to demonstrate some features of arsenic transport simulation. The column is 40 cm in height and 10 cm in diameter. The filter papers were placed at the bottom of the column as shown in **Fig. 4**. The column was filled to a height of 30 cm with the soil. The soil used in column experiment is a mixture of paddy field soil and air dried sediments of a spring collected from Munakata city, Fukuoka, Japan. Air dried sediment (5% of total weight of samples) was used to increase the amount of different chemical species, specifically Fe^{2+} concentration in the sample. The main physical and chemical properties of the soil used in this study are given in **Table 5**. Soil pH was measured in 1:2 soil to deionized water ratio. The top and the bottom of the column was closed using transparent resin plates with tubes for the flowing of influent and effluent, respectively. Tap water was used as influent. The main characteristics of the water are shown in **Table 6**.

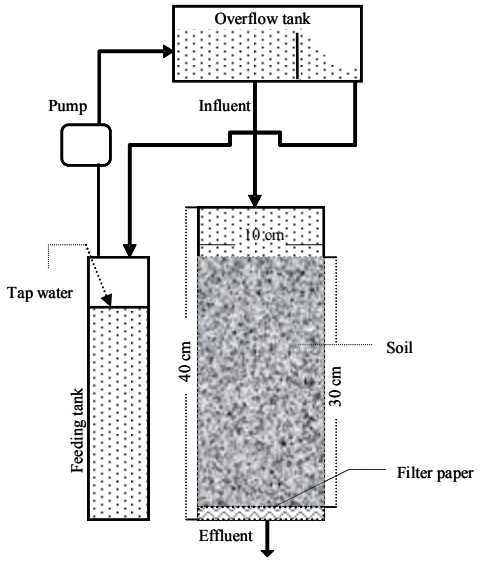

Fig. 4 Schematic diagram of the column experiment.

Table 5 Physiochemical properties of the soil.

Parameter	Values/Concentrations
Total Organic Carbon (wt. %)	1.95
pH	6.2
Ca (mg kg^{-1})	4160
Fe (mg kg^{-1})	39400
Mn (mg kg^{-1})	1130
As(III) (mg kg^{-1})	Below detection limit
As(V) (mg kg^{-1})	9.4
As_{total} (mg kg^{-1})	9.4

Table 6 Physiochemical characteristics of the tap water.

Parameter	Values/Concentrations
Conductivity (μS cm^{-1})	410
pH	7.9
ORP (mV)	301
As (μg L^{-1})	2.2
Fe (μg L^{-1})	1.6
Mn (μg L^{-1})	2.3

4. Results and Discussion

4.1 Simulation results

Figures 5(a) and **5(b)** show the results of simulated bacteria growth with depth. The top 10 cm of the column is dominated by bacterial group X_1 (facultative denitrificans), followed by bacterial group X_2 and X_3 (Mn(IV) and Fe(III) reducers). At the lower part of the column bacterial groups X_4 and X_5 (respiration bacteria of Fe-As compounds and As(V) reducers) tend to grow although their magnitude are still low compared to the bacteria X_1, X_2, and X_3. First few days the bacteria tend to be acclimated to the new environmental conditions.

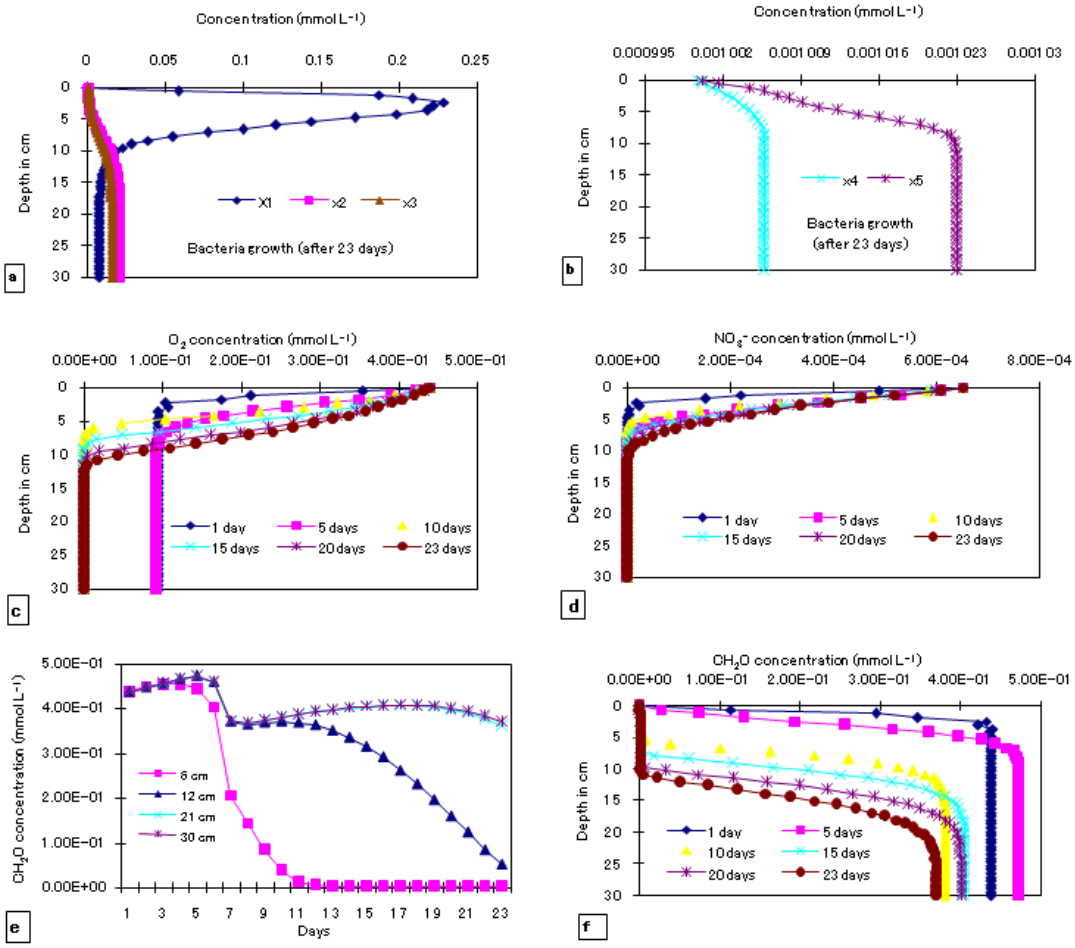

Fig. 5 Simulation results of (a) bacteria (X_1, X_2 and X_3) growth with depth, (b) bacteria (X_4 and X_5) growth with depth, (c) O_2 concentrations with depth, (d) NO_3^- concentrations with depth, (e) CH_2O concentrations with time and (f) CH_2O concentrations with depth.

Then the living bacteria population increases rapidly with time at an exponential growth in numbers, and the growth rate increasing with time. After that with the exhaustion of nutrients and secondary metabolic products, the growth rate has slowed to the point where the growth rate equals the death rate. **Figures 5(c)**, **5(d)**, and **5(f)** demonstrate the dependence of oxygen, nitrate, and organic carbon distribution with depth at different time and **Fig. 5(e)** shows the organic carbon distribution with time at different depths in mobile phase for soil column, respectively. The model simulation results show that the top 10 cm of soil are most important for oxygen, nitrate, and organic carbon consumption by micro-organism. Oxygen concentration reduced at the top (within 12 cm) of column and oxygen concentration decreased to zero after 7 days by aerobic bacterial group X_1. Denitrification occurred immediately following the reduction of oxygen by facultative bacterial group X_1. As long as the oxygen concentration exceeds 0.015mmol L^{-1}, the anaerobic

metabolism is inhibited. Afterwards the manganese reducer, iron reducer, respirative bacteria of Fe-As and arsenic reducer begin to grow, but their activity is limited by availability of Mn(IV), Fe(III), Fe-As compound and As(V). The organic carbon consumption by these bacteria is much smaller. Organic carbon increased at the top 6 cm of the column due to dissolved organic carbon from the soil matrix before bacterial group start to increase the population in adjustment period with the environment and then decreased due to use of facultative bacteria group. After 7 days and within 15 cm depths, the column becomes anaerobic due to O_2 and NO_3^- consumed by the facultative bacteria group and growth of bacteria decreased, so concentration of organic carbon increased to the column bottom.

4.2 Comparison between measured and simulated data

Manganese reducer in the model oxidizes CH_2O to carbon dioxide and reduces Mn(IV) from MnO_2 to Mn(II) ion. The most important model parameter was the exchange coefficient between solid Mn(IV) and microbially available Mn(IV) in the bio phase. The bacteria growth rate and exchange coefficient were tuned until the simulated manganese reduction resulted in the observed dissolved Mn(II) concentration became close. **Figure 6(a)** depicts good correlations of simulated manganese concentration with the measurement.

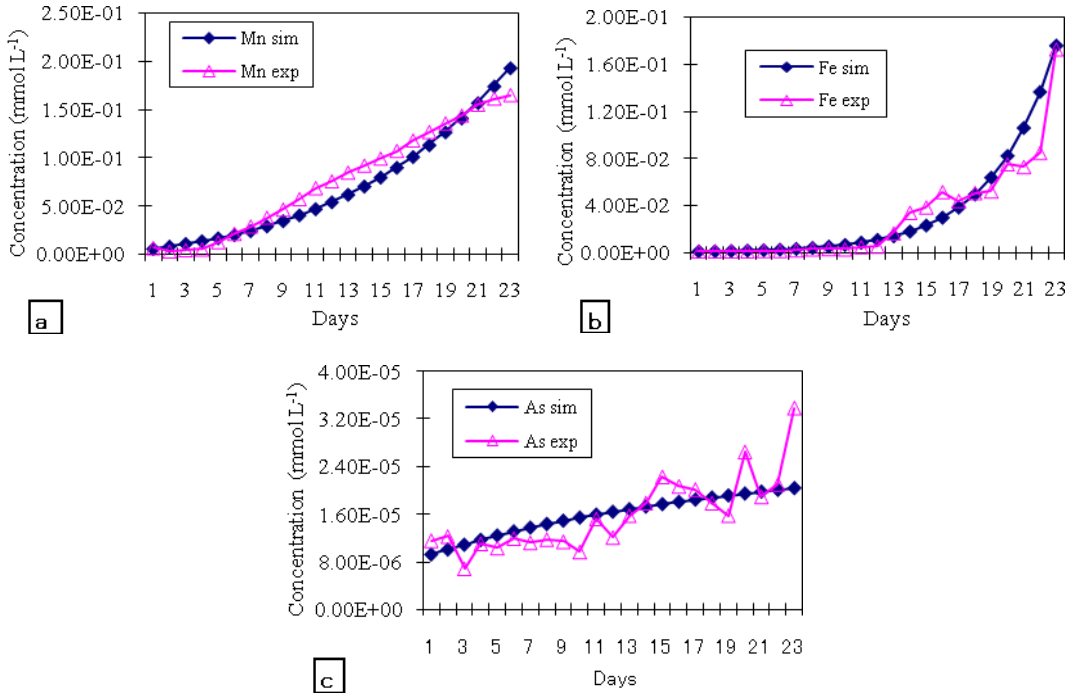

Fig. 6 Comparison of the measured concentrations of Mn, Fe, $As_{(total)}$ and CH_2O with those obtained from the microbially mediated biogeochemical model in (a), (b), (c) and (d) respectively.

The microbial Fe(III) reduction rate cannot directly be determined from observed dissolved Fe(II) concentration. Von Gunchten and Zobrist, (1993)[14] determined a microbial Fe(III) reduction rate in an additional column experiment, where no Fe-As compound was present. **Figure 6(b)** shows the observed and simulated Fe(II) content of the column at the end of the experiment (i.e., after 23 days of column operations). The measurements at the beginning of the column study showed Fe(II) content was about 1.30×10^{-3} mmol L^{-1}. After 23 days the mean Fe(II) concentration was increased to 1.72×10^{-1} mmol L^{-1}.

Figure 6(c) demonstrates that the simulated total arsenic concentrations are well agreed with the measured total arsenic concentrations. The most important model parameter was the exchange coefficient between solid Fe-As and microbially available Fe-As in the biophase. Again the bacteria

growth rate was tuned until the simulated arsenic concentration became close to the observed dissolved arsenic concentration.

5. Conclusions

A reactive transport model for describing the microbially mediated transformation of different contaminant and their subsequent transport was developed and tested using column experiment. The multi-component solute transport model is able to predict the behaviors of chemical species present arsenic rich aquifer under redox environment. In the model, initial arsenic in the soil was assumed as arsenic(V) concentrations because arsenic(III) concentration in the injected water was under detection limit. Increase of arsenic(V) concentration indicates that respiration bacteria of Fe-As starts to grow, it uses Fe-As compound as their metabolism to release iron(II) and arsenic (V). The released iron(II) by the respiration bacteria increase its concentration along with the iron(II) release by the iron reducing bacteria. Later arsenic(V) concentrations gradually decreased due to arsenic reducing bacteria uses this released arsenic(V) and changes it to arsenic(III). Under anoxic conditions, arsenate can serve as a terminal electron acceptor in the biological oxidation of organic matter.

The results of the present study demonstrate that the reducing geochemical condition of subsurface aquifer and arsenic in groundwater correlates well with DOC and with iron concentrations. Arsenic contents are well correlated with those of iron, manganese of soil sediments. The distribution of arsenic in subsurface soil sediments is controlled by different mineral and solid phases; and mobilization from different phases contributes to the total arsenic concentrations in groundwater. The present study also reports that the microbiological signatures of bacterial iron(III) reduction and arsenic release in groundwater. Bacteria-mediated mineralization of organic matter and reductive dissolution of Fe and Mn oxyhydroxide are considered to be the dominant processes to release arsenic. The simulation results of the model well matched those found experimentally. The proposed contaminant transport model can serve as a useful tool for predicting the fate and transport of arsenic, iron, manganese and other species in groundwater systems considering bacteria mediated oxidation and reduction bio-chemical processes.

Acknowledgements

The authors express the sincere gratitude to Japanese Society of Promotion Science for their financial support: *Simulation and remediation model for the groundwater contaminated by arsenic and multi-geochemical species*(No. 18-06396, 2006-2007).

References

1) Islam, F., Gault, A., Boothman, C., Polya, D., Charnock, J., Chatterjee, D., Lyond, J., 2004. Role of metal reducing bacteria in arsenic release from Bengal delta sediments. Nature 430, 68-71.
2) Newman, D.K., Ahmann, D., Morel, F.M.M., 1998. A brief review of microbial arsenate respiration. Geomicrobiol. J. 15, 255–268.
3) Lim, M., S., Yeo, I., W., Clement, T., P., Roh, Y., Lee, K., K. (2007). Mathemetical model for predicting microbial reduction and transport of arsenic in groundwater systems. Water Res. 41: 2079-2088.
4) Jennings, A.A., Kirkner, D.J., and Theis, T.L., (1982): Multicomponent equilibrium chemistry in groundwater quality models, Water Resources Research, Vol. 18, pp.1089-1096.
5) Schafer, D., Schafer, W. & Kinzelbach, W. (1998). Simulation of reactive processes related to biodegradation in aquifers. 1. Structure of the three dimensional reactive transport model. Cont. hyd. 31:167-186.
6) Lensing, H.J., Vogt, M., Herrling, B., (1994). Modeling of biologically mediated redox processes in the subsurface. Journal of hyd. 159, 125-143.
7) Schafer, D., Schafer, W. & Kinzelbach, W. (1998). Simulation of reactive processes related to biodegradation in aquifers. 2. Model application to a column study on organic carbon degradation. Cont. hyd. 31:187-209.

8) Widdowson, M.A., Molz, F.J., Benefield, L.D.,1988. A numerical transport model for oxygen and nitrate based respiration linked to substrate and nutrient availability in porous media.Water Resour.Res. 24, 1553-1565.
9) Kinzelbach, W., Schafer, W., Herzer, J., 1991. Numerical modeling of natural and enhanced denitrification processes in aquifers. Water Resour. Res. 27, 1123-1135.
10) Cummings DE, Caccavo F, Fendorf S & Rosenzweig RF (1999) Arsenic mobilization by the dissimilatory Fe(III)-reducing bacterium Shewanella alga. BrY. Environ. Sci. Technol. 33: 723–729.
11) Oremland, R.J., and Stolz, J.F (2005). Arsenic, microbes and contaminated aquifers. Trend in Microb. Vol.13 No.2 February.
12) Eljamal, O., Jinno, K. and Hosokawa, T.,(2007), Modeling of biologically mediated redox processes using sawdust as a matrix, Annual Journal of Hyd. Eng., JSCE, Vol.51, pp. 19-24.
13) Guerra, G., Jinno, K., Hiroshiro, Y. and Nakamura, K., (2004). Multi-component solute transport Model with cation exchange under redox environment and its application for designing the slow infiltration setup. Memoirs of the faculty of eng., Kyushu University, vol.64, no.1.
14) Von Gunten, U., Zobrist, J., 1993. Biogeochemical changes in groundwater-infiltration systems: column studies. Geochim. Cosmochim. Acta 57, 3895–3906.